Phase characteristics and elastic properties of binary Coulomb compounds

2003 J. Phys. A: Math. Gen. 36 6197

(http://iopscience.iop.org/0305-4470/36/22/348)

INSTITUTE OF PHYSICS PUBLISHING JOURNAL OF PHYSICS A: MATHEMATICAL AND GENERAL

J. Phys. A: Math. Gen. **36** (2003) 6197–6206 PII: S0305-4470(03)57122-0

Phase characteristics and elastic properties of binary Coulomb compounds

Takahiro Igarashi[1] **and Hiroshi Iyetomi**[2]

[1] Graduate School of Science and Technology, Niigata University, Niigata 950-2181, Japan
[2] Department of Physics, Niigata University, Niigata 950-2181, Japan

E-mail: hiro@phys.sc.niigata-u.ac.jp and hiyetomi@sc.niigata-u.ac.jp

Received 4 December 2002, in final form 24 February 2003
Published 22 May 2003
Online at stacks.iop.org/JPhysA/36/6197

Abstract

We have already shown that binary Coulomb compounds in disordered states are stabilized against phase separation in a minor ion rich region as charge asymmetry is enhanced; a stable phase appears approximately beyond the charge ratio $R_Z = 6$. In this paper, the mechanical properties of the stable compounds are elucidated through extensive calculations of the Coulomb energy increments due to virtual deformations. The compounds turn out to be much more isotropic than the mixed pure crystals in the linear response regime. And their effective elastic constants obtained by averaging over directions are well expressible in terms of those of the pure crystals. The compounds, however, show fragile behaviour at the degree of deformation where the pure crystal still retains its elasticity.

PACS numbers: 52.27.Gr, 97.60.Lf

1. Introduction

A binary ionic mixture (BIM) composed of two species of ions with different charges Z_1e and Z_2e is a prototype model for the interior of white dwarfs and the outer crust of neutron stars [1, 2]. The ions in the model are embedded in a uniform and rigid charge-compensating background with charge density ρ_e; throughout the present paper we assume the background has a unit volume. The typical central density of white dwarfs, consisting mainly of C and O, is around 10^6 g cm^{-3} and the Fe crust of neutron stars is assumed to have a density ranging from 10^4 to 10^7 g cm^{-3}. Under such high density conditions ions are completely ionized and the liberated electrons form a degenerate electron gas with a role of the ideal background; ions thereby interact with each other through bare Coulomb potentials.

Crystallization is predicted to happen upon cooling of dense stars. A one-component plasma crystallizes into a body-centred cubic (bcc) lattice and the transition point has been precisely determined by Monte Carlo simulations [3, 4]. In the BIM the phenomenon is much

more complicated emerging as an alloying problem. To simplify the situation, here we limit our attention to the ground state properties of BIMs. The ground state is characterized by the following two parameters. The one is a charge ratio R_Z defined as $R_Z \equiv Z_2/Z_1$; one can set $R_Z > 1$ without losing any generality. The remaining is a number fraction x given by $x \equiv N_2/N$, where $N \equiv N_1 + N_2$ is the total number of ions and N_i is the number of ions of species i.

Dyson [5] calculated the Madelung energies of BIMs in ordered solid states with specific compositions as a function of R_Z to find that some of them form stable compounds against phase separation. In particular, he discovered that a compound with the NaCl lattice structure was unusually stable around $R_Z = 13$; He^{+2}–Fe^{+26} BIM is a relevant system. He thereby pointed out a possibility that He ions may survive from nuclear burning in the Fe crust of neutron stars. Witten [6] developed this idea by including the zero-point energy and all first-order electronic screening effects. Foldy [7] elaborated on electrostatic stability of binary compounds with various kinds of lattice structures in equal concentration.

Ogata *et al* [8] extensively calculated the Madelung energies of BIMs in solid states with substitutional disorder for a range of $R_Z = 4/3$–4 to construct phase diagrams for various BIMs and ternary ionic mixtures at finite temperatures. The range of charge ratio pertains to possible plasmas realized in the interior of white dwarfs. The present authors [9] then expanded the accessible range of R_Z up to 13 to encompass the outer crust of neutron stars, and calculated the Madelung energies for BIM solids with interstitial disorder as well as substitutional disorder. Their remarkable finding is that the compounds in disordered states are also stabilized with the critical composition of $x_c \approx 0.2$ as the charge ratio is increased across $R_Z \approx 6$.

In this paper, we extend our previous work to elucidate the mechanical properties of stable BIMs in disordered solid states. These are essential physical inputs to analyse nonradial oscillations of neutron stars [10] and variable white dwarfs [11, 12]. The first-principle calculations of shear moduli for one-component Coulomb solids have been carried out at finite temperatures [13]. The phonon dispersion curves of the He–Fe compound of Dyson were calculated [6]; no appreciable mixing effects on its phonons were observed as compared to those of the corresponding pure Fe solid.

In passing we note that we are now much free to explore a wide variety of BIM solids, thanks to the recent success of crystallization of multicomponent non-neutral ion plasmas in a Penning trap; highly charged Xe ions were indirectly cooled to form a crystal through laser cooling of coexisting Be^+ ions [14].

2. Stability of disordered Coulomb compounds

We have considered BIMs with two representative disordered structures, that is, substitutional-type and interstitial-type alloys in the previous paper [9]. In order to construct such BIMs, we first prepared a crystalline system in which ions with larger charge were put in the bcc structure. We then randomly picked up some of the ions which were replaced by ions with smaller charge. Or we randomly inserted minor ions into interstitial sites of the bcc lattice of major ions. The former provides with a substitutional-type alloy and the latter, with an interstitial-type alloy. Finally, we carried out structural relaxations of the disordered BIMs, so prepared using the conjugate gradient method [15]. The stability of the Coulomb compounds was determined through comparison of their Madelung energies with those of the mixed pure crystals. This is one of the global minimization problems with many degrees of freedom so that it is important to make a good guess for the solution. In the calculations we used cubic cells containing a total of around 1000 ions. The minimization procedure was iterated until

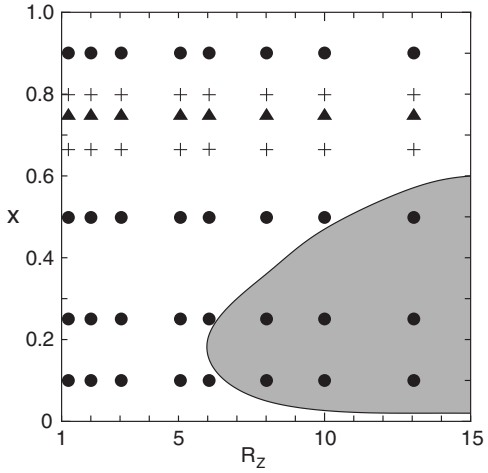

Figure 1. Stability diagram of disordered BIM solids in the R_Z–x plane. The solid triangles show the points where the computations were carried out only for BIMs with substitutional disorder; the crosses show the points only for BIMs with interstitial disorder; the solid circles refer to both types of disordered BIMs. The compounds are absolutely stable against phase separation in the dark region, while they are unstable outside. The critical point is located around $R_Z = 6$ and $x = 0.2$.

the relative variance of the energy reached 10^{-6}. The number of iterations varied from tens to hundreds depending on the initial arrangements.

Figure 1 illustrates a stability diagram of the disordered compounds along with computational points for the Madelung energies and the elastic constants. We especially note that a crossover from the substitutional disorder to the interstitial disorder as regards their relative stability takes place as R_Z is increased around $R_Z = 3$, although the Madelung energy of the stable compounds is virtually independent of which type of disorders is adopted at the onset of the structural relaxation in $R_Z > 2$.

The excess Madelung energies due to mixing for ordered and disordered AB_3-type compounds are plotted as a function of the charge ratio in figure 2. The disordered compound has a lower energy than the ordered compounds over the whole range of R_Z studied here. In contrast, as seen in figure 4 of [9] the disordered compound is not energetically favoured at $x = 0.5$; Dyson's compound with the NaCl structure is significantly more stable than the disordered one. But we assume that the formation of such a compound with a perfect crystalline structure may be difficult to be realized in the actual situations including rapid cooling of neutron stars. This assumption is supported by the computational evidence that the structural relaxation starting from totally different disorder arrangements leads to final states with similar energies. The construction of a phase diagram for the Coulomb compounds within the scope of disordered states may thus sound plausible from the dynamical point of view.

3. Elastic properties of disordered Coulomb compounds

The energy change of a cubic crystal with a unit volume due to arbitrary deformation is expressed [16] in the linear response as

$$\delta E = \tfrac{1}{2}C_{11}\left(u_{xx}^2 + u_{yy}^2 + u_{zz}^2\right) + C_{12}(u_{xx}u_{yy} + u_{yy}u_{zz} + u_{zz}u_{xx}) + 2C_{44}\left(u_{xy}^2 + u_{yz}^2 + u_{zx}^2\right) \qquad (1)$$

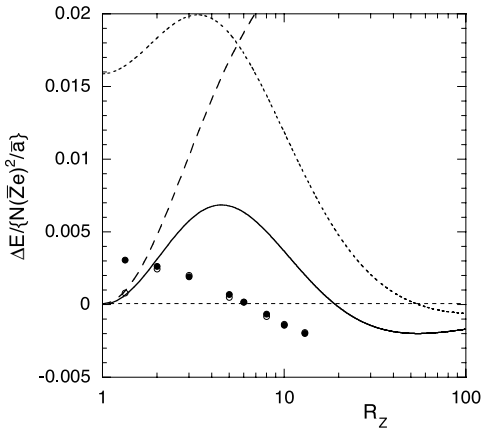

Figure 2. Excess Madelung energies due to mixing for various AB_3-type Coulomb compounds as a function of the charge ratio R_Z. The dotted, solid and dashed lines show the results for ordered compounds with the crystalline structures (a), (b) and (c) in figure 1 of [9], respectively. The solid and open circles show the results for the disordered compounds in interstitial and substitutional disorders, respectively. This is an amended figure of figure 2 in [9] where the results for the ordered compounds were erroneously multiplied by a factor of 2. Note that the energies are normalized here in terms of the averaged charge $\bar{Z}$ and averaged ion-sphere radius $\bar{a}$ in the same way as in the previous paper.

where u_{ij} is the strain tensor and $C_{\alpha\beta}$ is the elastic modulus tensor with $\alpha,\ \beta$ taking values from 1 to 6 in correspondence with xx, yy, zz, xy, yz, zx. Since the compounds in the rigid background are deformed with its total volume fixed (i.e., $\sum_i u_{ii} = 0$), we can rewrite (1) as

$$\delta E = B\left(u_{xx}^2 + u_{yy}^2 + u_{zz}^2\right) + 2C\left(u_{xy}^2 + u_{yz}^2 + u_{zx}^2\right) \tag{2}$$

where $\frac{1}{2}(C_{11} - C_{12})$ and C_{44} have been replaced with B and C. If the cubic symmetry is destroyed, elements for each direction of deformation must be distinguished:

$$\begin{aligned} B_{11} &= (2C_{11} - C_{12} - C_{31})/4 \\ B_{22} &= (2C_{22} - C_{23} - C_{12})/4 \\ B_{33} &= (2C_{33} - C_{31} - C_{23})/4. \end{aligned} \tag{3}$$

We define a directionally averaged value for B out of the individual elements $B_{11},\ B_{22}$ and B_{33}: $B = (B_{11} + B_{22} + B_{33})/3$. The same averaging procedure is followed for C. The elastic constants B_{11} and C_{44} for a pure Coulomb solid were obtained by Fuchs [17]. The results are 0.0245 and 0.1827 in units of $N(Ze)^2/a$ with $a = (-3Ze/4\pi\rho_e)^{1/3}$ where N ions of charge Ze are assumed to form a uniform bcc lattice in a neutralizing background with charge density ρ_e.

3.1. Elastic constants for mixed pure crystals

To extract intrinsic mixing effects on the elastic properties of the compounds, we define the elastic constants based on the linear mixing law $\eta_{\rm lm}$ (η denotes B or C) as

$$\eta_{\rm lm} = \eta_{\rm bcc}\left\{(1 - x) + x R_Z^{5/3}\right\} \tag{4}$$

where $\eta_{\rm bcc}$ is the corresponding constant of the pure bcc crystal of ionic species 1. The linear mixing values are equivalent to those of mixed pure crystals without interfacial energies between the two phases. The results at the computational points in figure 1 are listed in

Table 1. The elastic constants $B_{\rm lm}$ and $C_{\rm lm}$ of BIM solids based on the linear mixing law in units of $N(Z_1e)^2/a_1$, where $a_1 = (-3Z_1e/4\pi\rho_e)^{1/3}$.

	x						
R_Z	0.1	0.25	0.5	0.67	0.75	0.8	0.9
				$B_{\rm lm}$			
4/3	0.0260	0.0282	0.0320	0.0345	0.0358	0.0365	0.0380
2	0.0298	0.0378	0.0511	0.0600	0.0644	0.0671	0.0724
3	0.0373	0.0565	0.0886	0.110	0.120	0.127	0.140
5	0.0578	0.107	0.191	0.246	0.274	0.291	0.324
6	0.0705	0.139	0.254	0.331	0.370	0.393	0.439
8	0.100	0.214	0.404	0.530	0.594	0.632	0.708
10	0.135	0.302	0.580	0.766	0.859	0.914	1.02
13	0.198	0.458	0.892	1.18	1.32	1.41	1.58
				$C_{\rm lm}$			
4/3	0.193	0.210	0.238	0.257	0.267	0.272	0.283
2	0.222	0.282	0.381	0.447	0.480	0.500	0.540
3	0.278	0.422	0.661	0.820	0.900	0.948	1.04
5	0.431	0.804	1.42	1.84	2.04	2.17	2.42
6	0.526	1.04	1.90	2.47	2.76	2.93	3.27
8	0.749	1.59	3.01	3.95	4.43	4.71	5.28
10	1.01	2.25	4.33	5.71	6.40	6.82	7.65
13	1.47	3.41	6.65	8.81	9.89	10.5	11.8

table 1, where the elastic constants are normalized in terms of the physical parameters for ions of species 1. The mixing effects are discussed in reference to these results.

3.2. Elastic constants for disordered compounds

To obtain the elastic constants, we adopt the same deformations D_α ($\alpha = 1$–6) as in [13]:

$$D_1: \quad u_{xx} = \epsilon + \frac{3}{4}\epsilon^2 \qquad u_{yy} = u_{zz} = -\frac{\epsilon}{2}$$

$$D_2: \quad u_{yy} = \epsilon + \frac{3}{4}\epsilon^2 \qquad u_{zz} = u_{xx} = -\frac{\epsilon}{2}$$

$$D_3: \quad u_{zz} = \epsilon + \frac{3}{4}\epsilon^2 \qquad u_{xx} = u_{yy} = -\frac{\epsilon}{2}$$

$$D_4: \quad u_{xy} = u_{yx} = \frac{\epsilon}{2} \qquad u_{zz} = \frac{\epsilon^2}{4}$$

$$D_5: \quad u_{yz} = u_{zy} = \frac{\epsilon}{2} \qquad u_{xx} = \frac{\epsilon^2}{4}$$

$$D_6: \quad u_{zx} = u_{xz} = \frac{\epsilon}{2} \qquad u_{yy} = \frac{\epsilon^2}{4}$$

where ϵ is a perturbative parameter characterizing the degree of deformations. It is sufficient to keep the total volume of a system invariant up to order ϵ^2 in the linear response calculation. Substitution of each of the above deformations in equation (2) shows that the elastic constants can be calculated by taking the second derivative of the Madelung energy with respect to ϵ. The deformations D_α ($\alpha = 1$–3) represent uniaxial stretching of a cubic lattice along the principal axes and selectively yield the elastic constants $B_{\alpha\alpha}$. The remaining sets of deformations

Table 2. The elastic constants B and C in units of $N(Z_1e)^2/a_1$ for BIM solids in substitutional disorder. The numbers in parentheses denote possible errors in the last digits.

	x				
R_Z	0.1	0.25	0.5	0.75	0.9
			B		
4/3	0.0303 (0)	0.0379 (1)	0.0465 (3)	0.0471 (2)	0.0438 (1)
2	0.0777 (21)	0.166 (5)	0.238 (4)	0.228 (8)	0.125 (0)
3	0.174 (2)	0.271 (1)	0.422 (5)	0.567 (8)	0.422 (5)
			C		
4/3	0.191 (0)	0.204 (0)	0.229 (0)	0.259 (0)	0.280 (0)
2	0.190 (1)	0.195 (3)	0.255 (3)	0.377 (5)	0.504 (0)
3	0.185 (1)	0.277 (1)	0.436 (3)	0.602 (6)	0.852 (3)

Table 3. Same as table 2 but for BIM solids in interstitial disorder.

	x					
R_Z	0.1	0.25	0.5	0.67	0.8	0.9
				B		
3	0.182 (1)	0.273 (1)	0.427 (2)	0.570 (13)	0.564 (3)	0.383 (5)
5	0.250 (1)	0.478 (1)	0.804 (5)	0.936 (7)	0.918 (5)	0.787 (2)
6	0.338 (1)	0.648 (1)	1.09 (1)	1.27 (1)	1.24 (0)	1.06 (0)
8	0.483 (1)	0.979 (6)	1.57 (0)	1.89 (1)	1.82 (3)	1.59 (1)
10	0.605 (2)	1.34 (1)	2.06 (3)	2.57 (6)	2.50 (3)	2.25 (1)
13	0.953 (1)	1.95 (1)	2.81 (1)	3.62 (4)	3.58 (2)	3.46 (1)
				C		
3	0.180 (1)	0.276 (1)	0.434 (1)	0.618 (9)	0.894 (2)	1.27 (0)
5	0.253 (1)	0.515 (1)	0.990 (4)	1.71 (1)	2.59 (0)	3.62 (0)
6	0.342 (1)	0.698 (1)	1.34 (0)	2.32 (1)	3.52 (0)	4.91 (0)
8	0.484 (1)	1.08 (0)	2.24 (0)	3.88 (1)	6.00 (2)	8.51 (1)
10	0.687 (1)	1.56 (0)	3.34 (2)	5.78 (4)	9.00 (2)	12.9 (0)
13	0.952 (0)	2.42 (1)	5.38 (1)	9.27 (3)	14.5 (0)	20.9 (0)

D_α ($\alpha = 4$–6) represent skewing of the lattice in the principal planes leading to $C_{\alpha\alpha}$. We refer the readers to [13] for the computational details including handling of the long-range nature of Coulomb potentials through the Ewald summation.

The results for the averaged elastic constants B and C so obtained for BIM solids with substitutional and interstitial disorders are listed in tables 2 and 3, respectively. The tabulation takes into account the crossover in the relative stability between the two characteristic disorders around $R_Z = 3$. We find that B is always much larger than $B_{\rm lm}$. That is, the compounds show a much tougher response against the uniaxial deformation than the mixed pure crystals. In contrast, the compounds in the stable region are softer than the mixed pure crystals for the skew deformation. Combining these results we thus see that the anisotropy in the stable compounds is significantly reduced by the ionic mixing. The difference between B and C provides with a measure of mechanical anisotropy of a cubic crystal [16].

3.3. Effective shear modulus

The elastic properties of crystalline solids are generally anisotropic. But it is sometimes useful for practical purposes to introduce a directionally averaged value for the elastic constants.

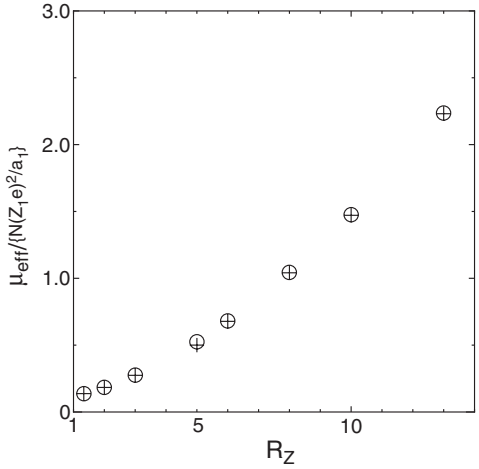

Figure 3. Effective shear modulus $\mu_{\rm eff}$ at $x = 0.25$ as a function of R_Z, measured by $N(Z_1e)^2/a_1$. The crosses are the results of disordered BIM solids. The results of BIMs with substitutional disorder are used for $R_Z \leqslant 3$, and those of BIMs with interstitial disorder are used for $R_Z \geqslant 5$. The open circles show the values of the linear mixing given by equation (3).

The effective shear modulus $\mu_{\rm eff}$ was thereby defined [13] as

$$\mu_{\rm eff} = (6B + 9C)/15. \tag{5}$$

For an isotropic body B, C and hence $\mu_{\rm eff}$ take the same value. The results in table 3 show that the anisotropy is significantly depressed by mixing for the compounds in the stable region. The results for $\mu_{\rm eff}$ actually calculated for the BIMs and those based on the linear mixing law are readily derived from tables 1, 2 and 3. We then see that those two results are almost indistinguishable, that is, there are no appreciable mixing effects on the averaged elastic properties of the stable compounds. This fact is demonstrated in figure 3 where $\mu_{\rm eff}$ are plotted as a function of R_Z at $x = 0.25$.

3.4. Nonlinear effects of deformation

To examine to what extent nonlinear effects are manifested on the mechanical properties of the compounds, we have directly calculated the Madelung energy for the compounds with varied deformations and compared the results with those of the linear response calculation given in the previous subsection. First we assess the nonlinear mechanical nature of a pure Coulomb lattice in the bcc structure. Figure 4 plots the variation of the Madelung energy of the system with respect to the degree of the D_4 deformation along with a parabolic curve derived from the Fuchs value for C. The elasticity is retained even at a level of 1% deformation. This will serve as a reference for the present discussion.

As demonstrated in figure 5(a), the compounds in the stable region near the critical point tend to easily lose the elasticity against the skew deformation; the compounds are fragile. This indicates that there exist a number of neighbouring states in the vicinity of the equilibrium state with similar Madelung energies. In contrast, figure 5(b) shows that the metastable compounds consisting dominantly of major ions are highly elastic over a wide range of deformation. Doping of minor ions into the lattice of major ions does not lead to softening of the elasticity. The same conclusions are drawn for the compounds with larger R_Z from the comparison in figure 6.

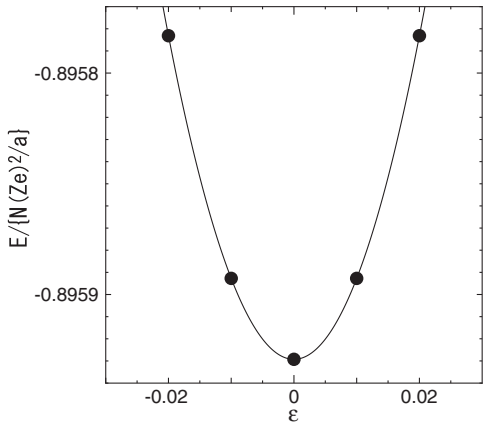

Figure 4. The Madelung energy in units of $N(Ze)^2/a$ of the pure bcc crystal as a function of the displacement ϵ in the deformation D_4. The parabolic curve is the linear response result with the Fuchs value for C.

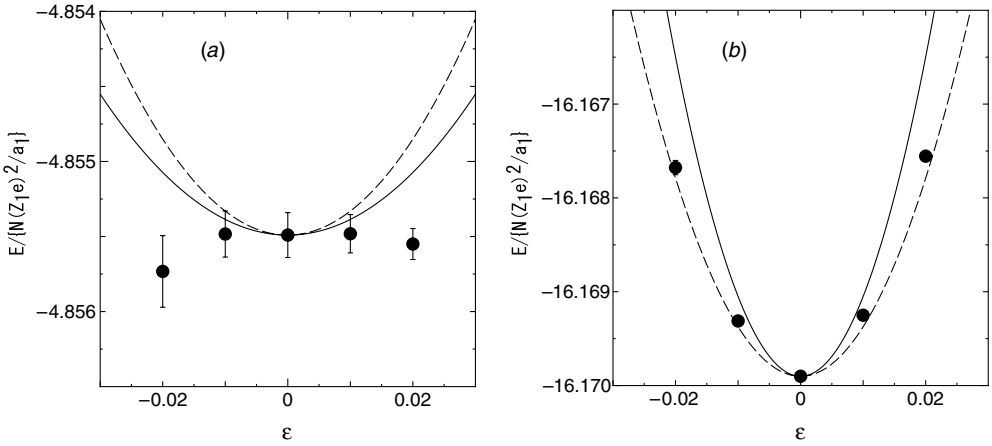

Figure 5. The Madelung energies in units of $N(Z_1e)^2/a_1$ of BIM solids with interstitial disorder for varied degrees of the D_4 deformation. Panel (a) shows the results for $R_Z = 8$ at $x = 0.25$; panel (b) shows the results for $R_Z = 8$ at $x = 0.9$. The solid lines and dashed lines show the parabolic curves derived from C and $C_{\rm lm}$, respectively. The solid circles show the values obtained by the direct calculations for deformed compounds. The errors were estimated out of three independent calculations.

Witten [6] calculated the phonon dispersions of the Fe bcc lattice and the He–Fe compound of Dyson with or without account for electron screening at equal charge density. He concluded that the elastic properties of the compound differ little from those of the pure lattice since the shear-wave curves are of roughly the same slope on the figures of the phonon dispersions. But he pointed out a possibility that nonlinear properties such as brittleness might be significantly different in compounds. To address his question we have also applied the present mechanical analyses to the He–Fe compound. The two elastic constants were obtained as $B = 3.65$ and $C = 4.84$ in the reduced units. The averaged value $\mu_{\rm eff}$ over propagating directions of phonons is almost identical to that of linear mixing where the pure Fe lattice gives a dominant contribution. This coincides with the pictorial observation due to him. Figure 7 shows that the

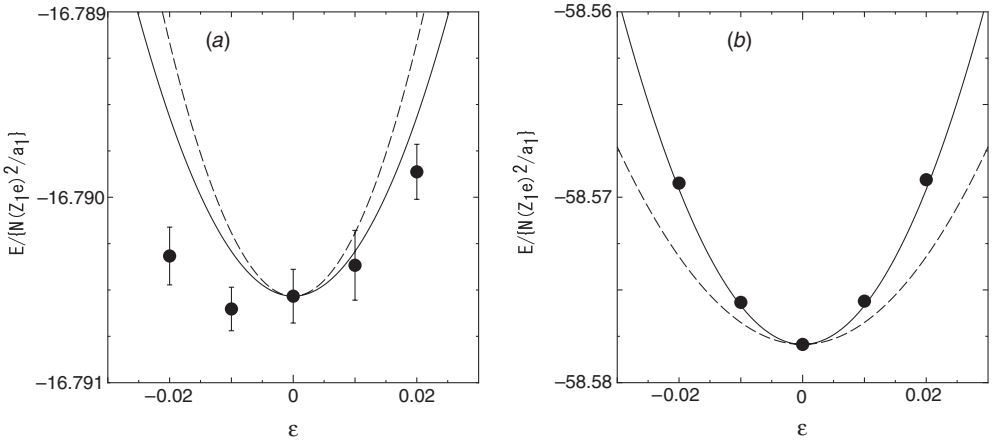

Figure 6. Same as figure 5, but for $R_Z = 13$.

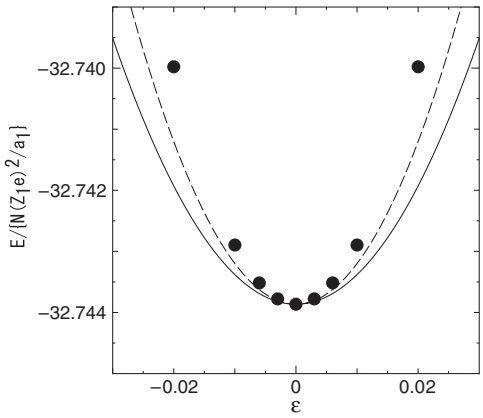

Figure 7. Same as figure 5, but for the He–Fe compound with the NaCl lattice structure ($R_Z = 13, x = 0.5$).

ordered compound is elastic as strong as the pure crystal. This gives an answer to the question posed by him.

4. Concluding remarks

We have carried out extensive calculations on the elastic properties of the disordered BIM solids. The effective shear modulus of the compounds in their stable region is virtually indistinguishable from that of the mixed pure crystals. The mixing effects, however, give rise to the nonlinear mechanical properties of the stable compounds such as fragility. As one of the possible extensions of the present study we are directed towards ternary compounds. Although standard white dwarfs evolved from main-sequence stars such as the sun consist mainly of C and O, it is assumed that they may contain heavier trace elements such as Ne and Fe [18]. Also it is predicted that more massive white dwarfs may form O–Ne–Mg cores [19]. Another way to proceed is towards trapped non-neutral plasmas of multi-ionic species [14].

One may be able to take advantage of the unusual stability of disordered Coulomb compounds to work out an efficient method of sympathetic cooling for highly charged ions.

Acknowledgment

This work has been supported by the JSPS Grants-in-Aid for exploratory scientific research with no 14658129.

References

[1] Baus M and Hansen J 1980 *Phys. Rep.* **59** 1
[2] Ichimaru S, Iyetomi H and Tanaka S 1987 *Phys. Rep.* **149** 91
[3] Ogata S and Ichimaru S 1987 *Phys. Rev.* A **36** 5451
[4] Stringfellow G S, DeWitt H E and Slattery W L 1990 *Phys. Rev.* A **41** 1105
[5] Dyson F J 1971 *Ann. Phys., NY* **63** 1
[6] Witten T A Jr 1974 *Astrophys. J.* **188** 615
[7] Foldy L L 1978 *Phys. Rev.* B **17** 4889
[8] Ogata S, Iyetomi H, Ichimaru S and Van Horn H M 1993 *Phys. Rev.* E **48** 1344
[9] Igarashi T, Nakao N and Iyetomi H 2001 *Contrib. Plasma Phys.* **41** 319
[10] Strohmayer T, Ogata S, Iyetomi H, Ichimaru S and Van Horn H M 1991 *Astrophys. J.* **375** 679
[11] Hansen C J and Van Horn H M 1979 *Astrophys. J.* **223** 253
[12] Winget D E, Kepler S O, Kanaan A, Montgomery M H and Giovannini O 1997 *Astrophys. J.* **487** L191
[13] Ogata S and Ichimaru S 1990 *Phys. Rev.* A **42** 4867
[14] Gruber L, Holder J P, Steiger J, Beck B R, DeWitt H E, Glassman J, McDonald J W, Church D A and Schneider D 2001 *Phys. Rev. Lett.* **86** 636
[15] Press W L, Flannery B P, Teukolsky S A and Vetterling W T 1989 *Numerical Recipes 'Fortran Version'* (Cambridge: Cambridge University Press) p 301
[16] Landau L D and Lifshitz E M 1986 *Theory of Elasticity* 3rd edn (Oxford: Butterworth-Heinemann) p 32
[17] Fuchs K 1936 *Proc. R. Soc.* A **153** 622
[18] Anders E and Grevesse N 1989 *Geochim. Cosmochim. Acta.* **53** 197
[19] Nomoto K and Hashimoto M 1988 *Phys. Rep.* **163** 13